Automotive Experiences
Vol. 5 No.2 (2022) pp. 137-149
p-ISSN: 2615-6202 e-ISSN: 2615-6636

Research Paper

Rollover Stability Analysis and Layout Optimization of a Delta E-trike

Fitri Endrasari[1], **Djati Wibowo Djamari**[1], **Bentang Arief Budiman**[2], **Farid Triawan**[1]

[1]Department of Mechanical Engineering, Sampoerna University, 12780, Indonesia
[2]Faculty of Mechanical and Aerospace Engineering, Institut Teknologi Bandung, 40116, Indonesia

djati.wibowo@sampoernauniversity.ac.id

https://doi.org/10.31603/ae.6136

Published by Automotive Laboratory of Universitas Muhammadiyah Magelang collaboration with Association of Indonesian Vocational Educators (AIVE)

Article Info
Submitted:
27/10/2021
Revised:
05/01/2022
Accepted:
07/01/2022
Online first:
09/03/2022

Abstract

This study derives a rollover index for a delta E-trike. Past works derive the rollover index by considering lateral centrifugal force only. In contrast, this study proposes a rollover index which is derived under the assumption that the centrifugal force act in both lateral and longitudinal direction. This assumption will give a result closer to the real-life application. In addition, a parametric study on the effect of center of gravity location on rollover index is also proposed. The study continued with the layout assessment, which is done as the considerations in rearranging the powertrain components inside the E-trike. The comparison between initial and new layout shows that the new arrangement gives several advantages to the delta E-trike.

Keywords: Rollover index; Center of gravity; Layout assessment

1. Introduction

Global warming is the gradual average Earth's surface temperature increment caused by greenhouse gases (GHG) emissions. Continuous global warming can cause an enormous climate change, which would be a massive disaster for all living things on Earth [1]. To prevent this, 197 parties concurred to adopt the Paris Agreement. It is a legally binding international treaty on climate change. Its goals are to keep the global average temperature at 2℃ over the pre-industrial level and limit the temperature increment to 1.5℃ [2]. Thus, those parties should control their GHG emissions. GHG includes carbon dioxide, methane, nitrous oxide, and fluorinated gases, with carbon dioxide as the primary contributor (about 65%) [3]. According to [4], 24% of carbon dioxide come from the energy sector and 74.5% is from road transportation. One of the suggested actions to reduce global emissions is vehicle electrification. Electric vehicles emit much less or even zero GHG compared to internal combustion engine vehicles [5].

Indonesia, as one of the parties on Paris Agreement, is one of the most populated country in the world. Its population growth results in increasing demand on road vehicles. Supporting vehicle electrification, Indonesian government created Program Kendaraan Bermotor Listrik Berbasis Baterai (KLBB) or battery electric vehicle (BEV) program which aims to implement BEV within its local government, ministerial, and state-owned and private enterprises. In addition, in 2019, the Presidential Regulation No. 55 of 2019 on Acceleration of Battery Electric Vehicles Program for Road Transportation is made [6]. This regulation aims to allow commercial and non-commercial incentives for local manufacturers with minimum rates of local components and charging infrastructure expansion. This regulation succeeds to attract several companies to start their investment in the battery and electric vehicle in Indonesia and have Indonesia as their target market. Those companies include Tesla, Hyundai Motor Group, LG Energy Solution, Contemporary Amperex Technology (CATL), Badische Anilin-und Soda-Fabrik (BASF), Toyota, and Honda [7].

Not only being the target market, but Indonesia also has a goal to lead and localize

battery and electric vehicle production. On March 2021, Indonesian government announced the development of Indonesia Battery Corporation (IBC) [8]. It is a combination of PT Indonesia Asahan Aluminium (Persero)/Inalum or MIND ID, PT Pertamina (Persero), and PT PLN (Persero). This corporation will focus on the battery and electric vehicle development. Besides IBC, Indonesia also has National Center of Excellence on Sustainable Transportation Technology (NCSTT). NCSTT is an individual research center at Bandung Institute of Technology (ITB) to encourage, support, and conduct applied engineering and technology for transportation system. It is appointed by the Indonesian Ministry of Research, Technology, and Higher Education as the host for the national center of excellence for transportation. To support the Indonesian government on the vehicle electrification, NCSTT has been developing several products. One of its under-development products is a cargo three-wheeled vehicle or E-trike for urban logistics. **Figure 1** shows the cargo E-trike by NCSTT.

Figure 1. E-trike by NCSTT

There are several advantages of using E-trike as urban logistic vehicle over a car. E-trike needs less energy to move because it has only three wheels and, usually, lighter [9]. It means, with the same battery capacity as car, E-trike can travel longer and farther. Also, its smaller size compared to a car can be a solution for traffic congestion [10]. Even though E-trike is mostly smaller, it still provides the users enough space to carry logistics. Shown in **Figure 1**, the cargo E-trike developed by NCSTT employs delta configuration, where it has one wheel at the front and two wheels at the rear. Another three-wheeled vehicle configuration is called tadpole, where it has two wheels at the front and one wheel at the rear.

For urban logistic vehicle, the delta configuration has some advantages compared to the tadpole configuration. The delta configuration has higher maneuverability and is more versatile [11]. Moreover, a cargo vehicle needs to have some space at the rear part. For this purpose, the delta configuration has simpler layout configuration. Not only for space, but it also makes the delta configuration more economical. However, the delta configuration has one drawback, which is its rollover tendency. Compared four-wheeled car and there-wheeled vehicle with tadpole configuration, the delta configuration has the highest rollover tendency [10]. Vehicle rollover might occur under several circumstances such as road condition, tripping, speeding, and so on [12]. The tendency of a vehicle to rollover is inversely proportional to the speed that the vehicle can have when turning. Having high rollover tendency means the three-wheeled vehicle with delta configuration has small turning velocity. Therefore, rollover stability analysis becomes very critical for E-trike with delta configuration.

Many studies on rollover stability analysis of three-wheeled vehicle with delta configuration have been done. Those studies analyzed the rollover stability of a three-wheeled vehicle by assuming that the centrifugal force acts only in the lateral direction [10], [13], [14]. Centrifugal force exists when a vehicle is turning. It pulls the vehicle out from the center of rotation. In real situation, the centrifugal force acts in both lateral and longitudinal direction of the vehicle.

The rollover index, RI, for a delta E-trike can be derived using the general form for rollover index shown in (1), where F_{ZL} and F_{ZR} are the normal forces acting on the left- and right-rear tire, respectively. A vehicle will rollover when its rollover index is less than -1 or more than 1. Several studies on the stability of a delta vehicle have been done [10], [13], [14]. Those studies assumed that the centrifugal force acts only in the lateral direction, which actually exists in the lateral and longitudinal direction. They also focus

only on the factors that affect the stability of the delta vehicle without considering the layout design. With respect to the previous studies, this study has three main contributions: 1) derives rollover index using the real configuration of centrifugal force which has both lateral and longitudinal component, 2) perform a parametric study on how the center of gravity location affecting the E-trike's rollover index, 3) performs layout assessment to propose a layout design consideration for the E-trike, and 4) proposes a new layout for the NCSTT's E-trike. The new layout is, theoretically, proven to give a better environment for the powertrain components inside the E-trike and increase the E-trike's stability during a turn. In general, the result of this study is expected to have a contribution in green vehicle, especially for E-trike with delta configuration.

$$RI = \frac{F_{ZL} - F_{ZR}}{F_{ZL} + F_{ZR}} \quad (1)$$

2. Problem Statement and Methodology

2.1. *Problem Statement*

In this work, a rollover index for a delta E-trike during a turn will be derived. **Figure 2** shows the schematic of a delta E-trike in a turn.

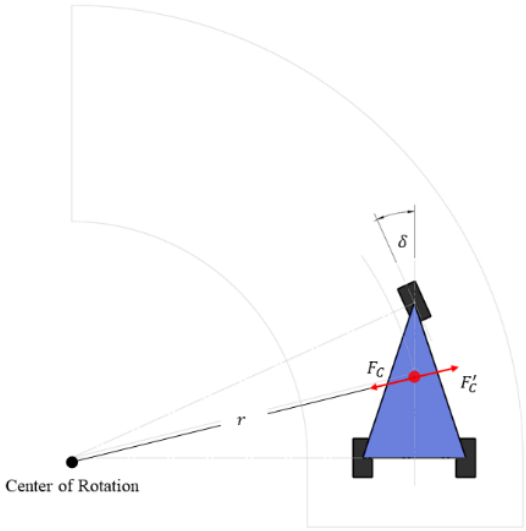

Figure 2. The turning mechanism of a delta E-trike

The E-trike is modeled as a rigid body with mass m. During a turn, a centrifugal force is generated. It pulls the E-trike out from the center of rotation and can cause the E-trike to rollover. The centrifugal force is highly proportional to the turning velocity. It means, higher velocity increases the possibility of the E-trike to roll over. The rollover index derivation in this study is derived under the real configuration of centrifugal force which act in both lateral and longitudinal direction.

Rollover index is affected by the center of gravity location, which also shown in this study. Therefore, optimizing the turning velocity that the E-trike can have, a layout assessment is done. Not only for an E-trike, but the layout assessment done in this study also applicable for other electric vehicles as it is conducted generally. The consideration from the layout assessment will be used to rearrange the powertrain components inside the E-trike by means to change its center of gravity location. At the end, a comparative analysis between initial and new layout is done to show the advantages of the proposed layout.

2.2. *Methodology*

In general, this study is done under three methods:

1. **Rollover index derivation**. This process includes the derivation of the rollover index of a delta E-trike with real centrifugal force configuration.
2. **Parametric Study of Rollover Index.** This section is the study on how each parameter to form the center of gravity (T_1, L_1, and Z) affect the rollover index of a delta E-trike.
3. **Layout Assessment.** This process is done to collect the consideration(s) needed in powertrain components placement.

The methodology above will solve the problems stated in Section 2.1. The rollover index derivation will show us the parameters that affect the stability of the E-trike. This derivation uses free-body diagrams of the E-trike to get the normal forces that act on rear tires, F_{ZL} and F_{ZR}, which are the variables needed to determine the rollover index. Then, the parametric study will closely identify the effect of the center of gravity location on the E-trike's rollover index. It also analyzes how its allowable turning velocity is affected by it. Finally, considering that the center of gravity location is highly related to the mass distribution within the E-trike, the layout assessment will acknowledge the consideration(s) needed for the placement of the powertrain components. This assessment will be used for layout optimization.

2.2.1. *Rollover Index Derivation*

To derive the rollover index, free-body diagrams (FBDs) of delta vehicle from back, side, and top view are made. Then, moment equilibrium equations are derived from these FBDs. **Figure 3** shows the FBD of the delta E-trike viewed from the back. F_{ZL}, F_{ZR}, and F_{ZF} are the normal force on the left-rear, right-rear, and front wheels, respectively. F_{XL}, F_{XR}, and F_{XF} are the lateral forces acting on the left-rear, right-rear, and front wheels, respectively. O_L and O_R are the contact points on the left-rear and right-rear wheels, T_1 and T_2 are the distance from the center of gravity to the left wheel and right wheel in the x axis (lateral axis), respectively and $T = T_1 + T_2$ is the wheel track. Meanwhile, m is the total mass of the vehicle, g is the gravitational acceleration, and F_{cx} is the centrifugal force component in the lateral direction.

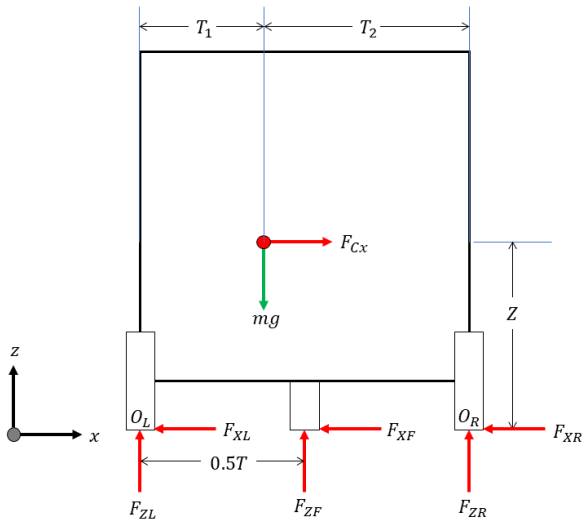

Figure 3. The back viewed FBD of a delta vehicle

Based on the FBD from **Figure 3**, F_{Z_L} and F_{Z_R} can be obtained from the derivation of moment equilibrium equations with respect to Point O_L and O_R. First, the moment equilibrium equation with respect to Point O_L is derived to obtain F_{Z_R}.

$$\sum M_{O_L} = 0$$
$$-mgT_1 - F_{Cx}Z + F_{ZF}0.5T + F_{ZR}T = 0$$
$$F_{ZR}T = mgT_1 + F_{Cx}Z - 0.5F_{ZF}T$$

$$F_{ZR} = mg\frac{T_1}{T} + F_{Cx}\frac{Z}{T} - 0.5F_{ZF} \qquad (2)$$

Next, the moment equilibrium with respect to Point O_R is derived to obtain F_{Z_L}.

$$\sum M_{O_R} = 0$$
$$-F_{ZF}\frac{T}{2} - F_{Cx}Z + mgT_2 - F_{ZL}T = 0$$
$$F_{ZL}T = mgT_2 - F_{Cx}Z - 0.5F_{ZF}T$$

$$F_{ZL} = mg\frac{T_2}{T} - F_{Cx}\frac{Z}{T} - 0.5F_{ZF} \qquad (3)$$

To obtain RI, there should not be unknown variable. Thus, F_{ZF} should be replaced with other known parameter(s). This can be done by deriving the moment equilibrium equation of the E-trike using side point of view. **Figure 4** shows the delta E-trike viewed from the right. F_{ZL}, F_{ZR}, and F_{ZF} are the normal force on the left-rear, right-rear, and front wheels, respectively. F_{YL}, F_{YR}, and F_{YF} are the trolling resistance acting on the left-rear, right-rear, and front wheels, respectively. O and A are the contact points on the rear and front wheels, L_1 and L_2 are the distance from the center of gravity to the front and the rear axle in the y axis (longitudinal axis), respectively and $L = L_1 + L_2$ is the wheelbase. Meanwhile, m is the total mass of the vehicle, g is the gravitational acceleration (9.81 m/s), F_{cy} is the centrifugal force component in the longitudinal direction and a_L is the longitudinal acceleration.

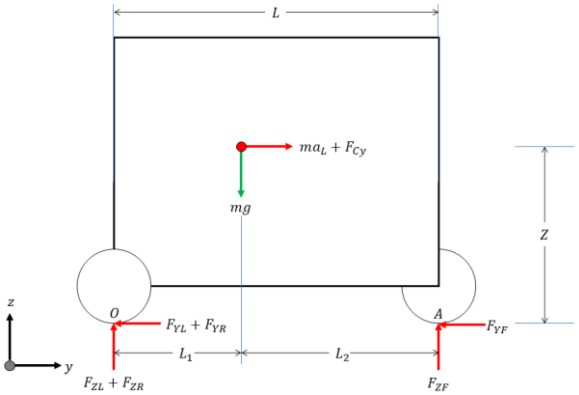

Figure 4. The side viewed FBD of a delta vehicle

From **Figure 4**, F_{ZF} can be obtained from the derivation of moment equilibrium with respect to Point O.

$$\sum M_O = 0$$
$$-mgL_1 - (ma_L + F_{Cy})Z + F_{ZF}L = 0$$

By assuming constant velocity, $a_L = 0$. Therefore:

$$-mgL_1 - F_{Cy}Z + F_{ZF}L = 0$$
$$F_{ZF}L = mgL_1 + F_{Cy}Z$$

$$F_{ZF} = \frac{mgL_1 + F_{Cy}Z}{L} \quad (4)$$

Substitute (2) and (3) to the general RI equation, we get:

$$RI = \frac{mg\frac{T_2}{T} - F_{Cx}\frac{Z}{T} - 0.5F_{ZF} - mg\frac{T_1}{T} - F_{Cx}\frac{Z}{T} + 0.5F_{ZF}}{mg\frac{T_2}{T} - F_{Cx}\frac{Z}{T} - 0.5F_{ZF} + mg\frac{T_1}{T} + F_{Cx}\frac{Z}{T} - 0.5F_{ZF}}$$

Or,

$$RI = \frac{mg\left(\frac{T_2 - T_1}{T}\right) - 2F_{Cx}\frac{Z}{T}}{mg\left(\frac{T_2 + T_1}{T}\right) - F_{ZF}}$$

For $T_2 + T_1 = T$, and $F_{ZF} = \frac{mgL_1 + F_{Cy}Z}{L}$, the equation above becomes:

$$RI = \frac{mg\left(\frac{T_2 - T_1}{T}\right) - 2F_{Cx}\frac{Z}{T}}{mg - \frac{mgL_1 + F_{Cy}Z}{L}} \quad (5)$$

The turning radius, r, is a function of the turning angle δ. This can be examined by observing the E-trike from above during a turn. The top-view of E-trike during a left-turn is given in **Figure 5**, where l, s, and q are the distance from the center of gravity, center of the vehicle, and the front wheel to the center of rotation C, respectively. α and ψ are the angle between the lateral and longitudinal axis and the turning radius r, respectively. β is the angle between r and q, γ is the angle between the longitudinal axis and q, and v is the turning velocity. F_C is the centrifugal force, F_{TL} and F_{TR} are the tractive force on left and right tires; F_{YL}, F_{YR}, and F_{YF} are the rolling resistance on left, right, and front tires; F_{XR}, F_{XL}, and F_{XF} are the lateral forces on left, right, and front tires. The tractive forces, rolling resistance, and lateral forces are such that the E-trike undergoes a steady state turning; and they are drawn in **Figure 5** to complete the free-body diagram.

Based on the schematic in **Figure 5**, we get the following equations:

$$F_{Cx} = F_C cos\alpha \quad (6)$$

$$F_{Cy} = F_C sin\alpha \quad (7)$$

$$\alpha + \beta = \delta \quad (8)$$

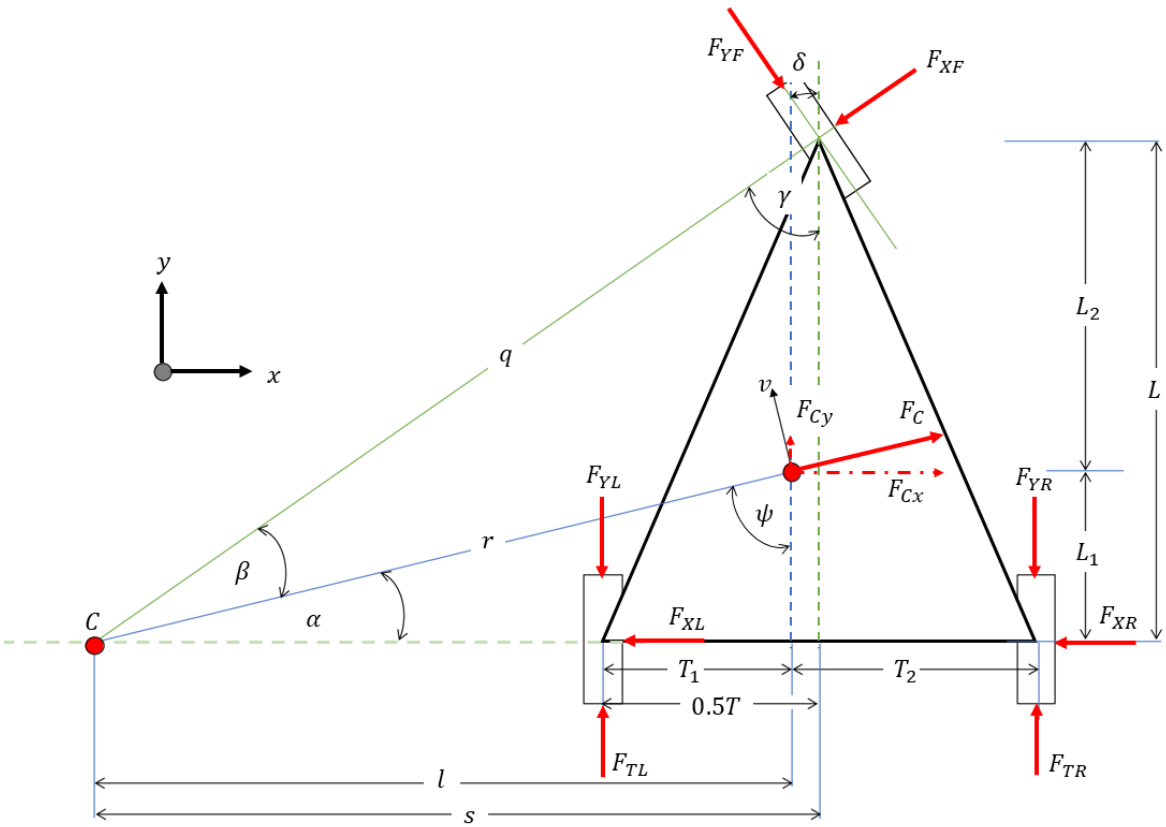

Figure 5. Top-viewed FBD of a delta vehicle during a steady-state turn

Using Sine rule, the angle and the sides of the triangle in **Figure 5** can be correlated as follows:

$$\frac{L}{\sin(\alpha+\beta)} = \frac{L}{\sin(\delta)} = \frac{q}{\sin(90°)} = \frac{s}{\sin(\gamma)}$$

$$\frac{L_1}{\sin(\alpha)} = \frac{r}{\sin(90°)} = \frac{l}{\sin(\psi)}$$

$$sin\ (90°) = \frac{qsin(\delta)}{L}$$

$$sin\ (90°) = \frac{rsin(\alpha)}{L_1}$$

$$\frac{rsin(\alpha)}{L_1} = \frac{qsin(\delta)}{L}$$

Thus,

$$r = \frac{qL_1 \sin\ (\delta)}{Lsin(\alpha)} \tag{9}$$

Then, using the trigonometric relationship, $\sin(\delta) = \frac{L}{q}$ and $\tan\ (\alpha) = \frac{L_1}{l}$. Therefore,

$$q = \frac{L}{\sin\ (\delta)} \tag{10}$$

$$\alpha = \tan^{-1}\left(\frac{L_1}{l}\right) \tag{11}$$

Let $l' = \frac{1}{2}T - T_1$, the schematic in **Figure 4** also shows that $l = s - l'$ and $\tan(\delta) = \frac{L}{s}$. Thus, $s = \frac{L}{\tan(\delta)}$ and $l = \frac{L}{\tan\ (\delta)} - 0.5T + T_1$. Therefore,

$$\alpha = \tan^{-1}\left(\frac{L_1}{\frac{L}{\tan(\delta)} - 0.5T + T_1}\right) \tag{12}$$

By substituting equations (10) and (12) into (9), we obtain:

$$r = \frac{\frac{L}{\sin(\delta)} L_1 \sin(\delta)}{Lsin\left(\tan^{-1}\left(\frac{L_1}{\frac{L}{\tan(\delta)} - 0.5T + T_1}\right)\right)}$$

$$\alpha = \tan^{-1}\left(\frac{L_1}{\frac{L}{\tan(\delta)} - 0.5T + T_1}\right) \tag{13}$$

Then, substitute (6) and (7) into (5), we have:

$$RI = \frac{mg\left(\frac{T_2 - T_1}{T}\right) - 2F_C \cos(\alpha)\frac{Z}{T}}{mg - \frac{mgL_1 + F_C \sin(\alpha)Z}{L}}$$

Let $F_C = \frac{mv^2}{r}$, the magnitude of the centrifugal force, RI can be written as:

$$RI = \frac{mg\left(\frac{T_2 - T_1}{T}\right) - 2m\frac{v^2}{r}\cos(\alpha)\frac{Z}{T}}{mg - \frac{mgL_1 + m\frac{v^2}{r}\sin(\alpha)Z}{L}}$$

By eliminating m from the above equation:

$$RI = \frac{L}{T}\frac{r(T_2 - T_1) - 2v^2 Zcos(\alpha)}{grL_2 - v^2 Zsin(\alpha)}$$

Then, by substituting α and r in equation above using (12) and (13), we finally obtain (Equation 14).

Equation (14) shows that for a delta vehicle, the rollover index is affected by the center of gravity location, dimension of the vehicle, turning velocity, and turning angle. It also shows that the rollover index is affected by the ratio between the wheelbase and wheel track of the vehicle.

$$RI = \frac{L}{T}\frac{\left(\frac{L_1}{sin\left(\tan^{-1}\left(\frac{L_1}{\frac{L}{\tan(\delta)} - 0.5T + T_1}\right)\right)}\right)(T - 2T_1) - 2v^2 Zcos\left(\tan^{-1}\left(\frac{L_1}{\frac{L}{\tan(\delta)} - 0.5T + T_1}\right)\right)}{g\left(\frac{L_1}{sin\left(\tan^{-1}\left(\frac{L_1}{\frac{L}{\tan(\delta)} - 0.5T + T_1}\right)\right)}\right)(L - L_1) - v^2 Zsin\left(\tan^{-1}\left(\frac{L_1}{\frac{L}{\tan(\delta)} - 0.5T + T_1}\right)\right)} \tag{14}$$

2.2.2. *Parametric Study of Rollover Index*

In the Section 2.1, (14) shows that the rollover index of E-trike is affected by its dimensions and the value of T_1, L_1, Z, v, g, and δ. Therefore, in this section, a parametric study is done to furtherly analyzed the effect of center of those variables on rollover index. By assuming $g = 9.81$ m/s, the parametric study is done by changing the value of T_1, L_1, and Z for $10^{\circ} \leq \delta \leq 28^{\circ}$ and $1.0 \leq v \leq 2.0$ m/s. This analysis is done by using MATLAB. In this analysis, the parameters of the E-trike by NCSTT, which tabulated on **Table 1** and **Table 2** are used.

Based on the parameters in **Table 1**, the following range are used in the parametric study:

$0 \leq T_1 \leq 0.8$ m

$0.31 \leq L_1 \leq 1.88$ m

$0 \leq Z \leq 1.68$ m

Table 1. Parameters of the E-trike by NCSTT

Parameter of E-trike	Notation	Value
Total mass	m	350.57 kg
Track width	T	0.8 m
Wheelbase	L	1.87954 m
Height	H	1.67732 m
Radius of the wheel	R_w	0.2455 m
Width of the wheel	W_w	0.150 m

Table 2. Initial center of gravity location of the E-trike by NCSTT

CoG Parameter	Reference	Notation	Value
CoG on x-axis	Left-Rear Wheel	T_1	391.24
CoG on y-axis	Rear Axle	L_1	822.89
CoG on z-axis	Ground	Z	635.33

2.2.3. *Layout Assessment*

The center of gravity location correlates with the mass distribution within a vehicle. Since the rollover index for a vehicle is affected by the center of gravity location, a layout assessment is needed to know the layout design consideration for the components inside the vehicle. In an electric vehicle, the mass distribution is mainly affected by its powertrain components distribution. Those components include the battery pack, battery management system (BMS), inverter, and electric motor. While operating, those components generate heat. The ongoing usage might lead to overheating, which can cause performance degradation or even thermal runaway [15], [16]. To keep the ambient temperature within the tolerated range, they should be placed in an area with swift air circulation.

Besides temperature, the powertrain components are also sensitive to vibration, especially the electric motor [17]. Fatigue failure on electrical components due to vibration is a common problem in electric vehicles. It is even one of the top five causes of failure for electric motor. Therefore, it is crucial to put those components on an area with low vibration. While other components can be located on various locations, battery pack is usually located either at the lower-center or rear part of an electric vehicle [18], [19]. Placing the battery pack at the lower-center part of the vehicle decreases the vibration that it experiences compared to the battery placement at the rear part of the vehicle. However, placing the battery pack at the rear part of the vehicle will provide the battery a better air circulation, which can prevent thermal runaway within the battery pack.

3. Results and Discussions

3.1. *Effect of Center of Gravity Location on Rollover Index*

3.1.1. *Effect of T_1*

The analysis on the effect of center of gravity location on rollover index is started with the analysis on the effect of T_1. **Figure 6** show the RI value when T_1 values are varied. The graphs show that the range of the rollover index gets bigger as the turning velocity and angle increase. They also show that T_1 has negative linear relationship with the rollover index.

3.1.2. *Effect of L_1*

Figure 7 show the rollover index of E-Trike when L_1 values are varied. The results show that the rollover index is either increases or decreases as the center of gravity location is moved forward. Thus, the center of gravity should be located as close as possible to the rear axle to increase the vehicle's rollover stability.

3.1.3. *Effect of Z*

Lastly, the analysis on the effect of Z value is done. **Figure 8** show the rollover index of E-Trike when Z is varied. They show that the rollover index decreases as the center of gravity location is higher. Thus, the center of gravity should be located as low as possible to increase the vehicle's rollover stability.

3.2. *Optimum Center of Gravity Location Associated with Rollover Index*

Based on **Figure 6** to **Figure 8**, an optimum center of gravity associated with the rollover index is proposed. For T_1, **Figure 6** show that the rollover index is close to 0 (good rollover's stability) when the center of gravity is in the middle of the E-trike laterally ($T_1 = 0.5T$). Thus, the suggested T_1 value is 0.4 m measured from the left-rear tire. For L_1, considering the natural characteristic of center of gravity that divides the mass of the front and rear part equally, the suggested value for L_1 is 0.7 m. For Z, the smallest rollover index exists when $Z = 0$ m. However, this value is impossible to be realized since it means that the center of gravity is located exactly on the ground. Also, there is also speed bump on some roads which should be carefully considered. In Indonesia, based on the Ministry of Transportation Decree/Regulation No. 3 Year 1993 about Controlling and Safety Equipment for Road Users, the shape of speed bumper should be isosceles trapezoid with maximum height of 12 cm. Beside the range from the graph, the ground clearance for several cars is also considered. The chosen value for the ground clearance is 0.165 m [20]. Considering the mass distribution inside the E-trike, it is impossible to have the Z value exactly at 0.165 m. Thus, the possible value for Z would be from about 0.3 to 1.0 m. It is to note that the actual values of T_1, L_1, and Z depend on the possible layout arrangement of E-trike itself.

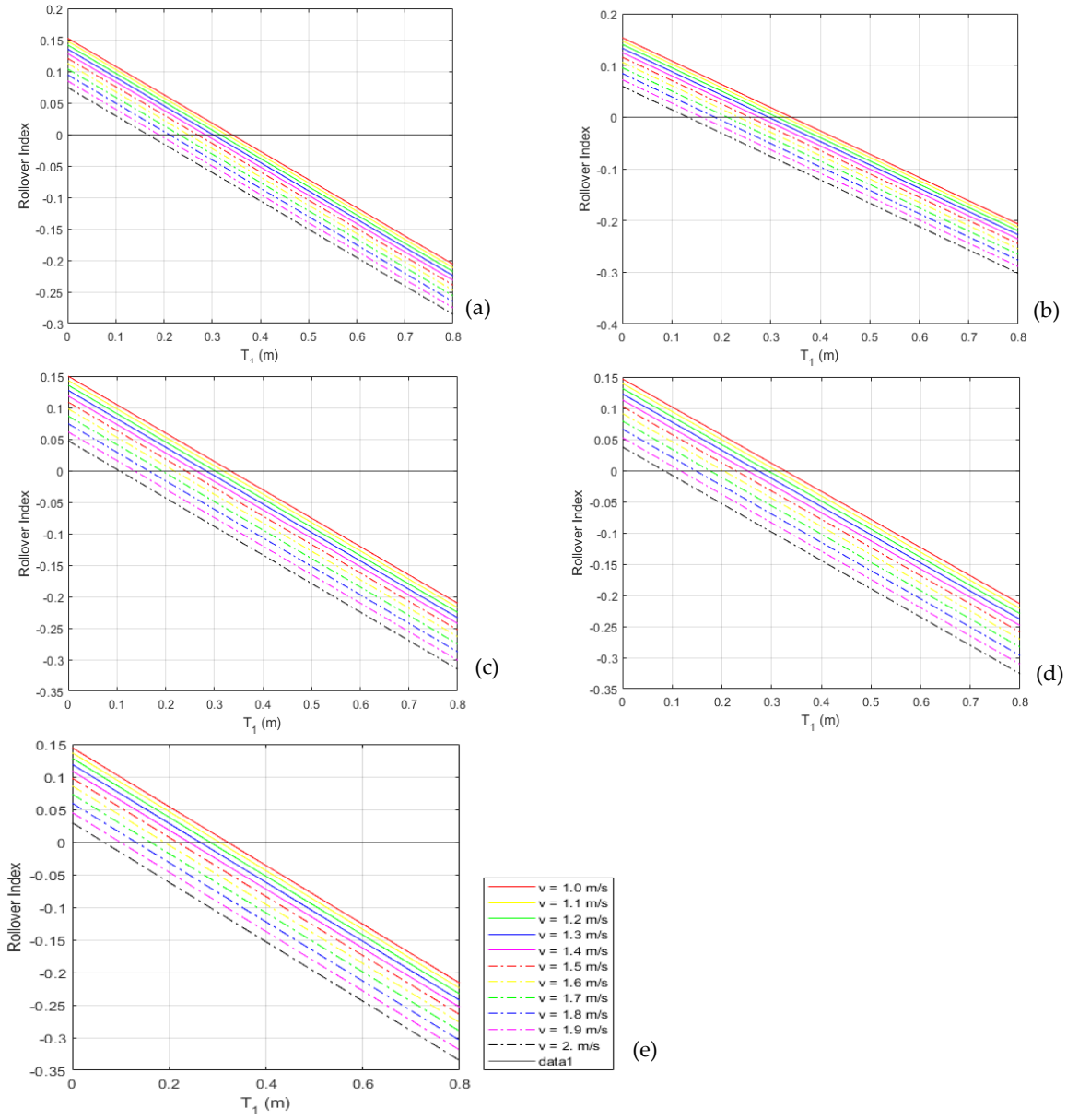

Figure 6. Rollover Index vs. T_1 for (a) $\delta = 10^{\circ}$; (b) $\delta = 15^{\circ}$; (c) $\delta = 20^{\circ}$; (d) $\delta = 25^{\circ}$; (e) $\delta = 28^{\circ}$

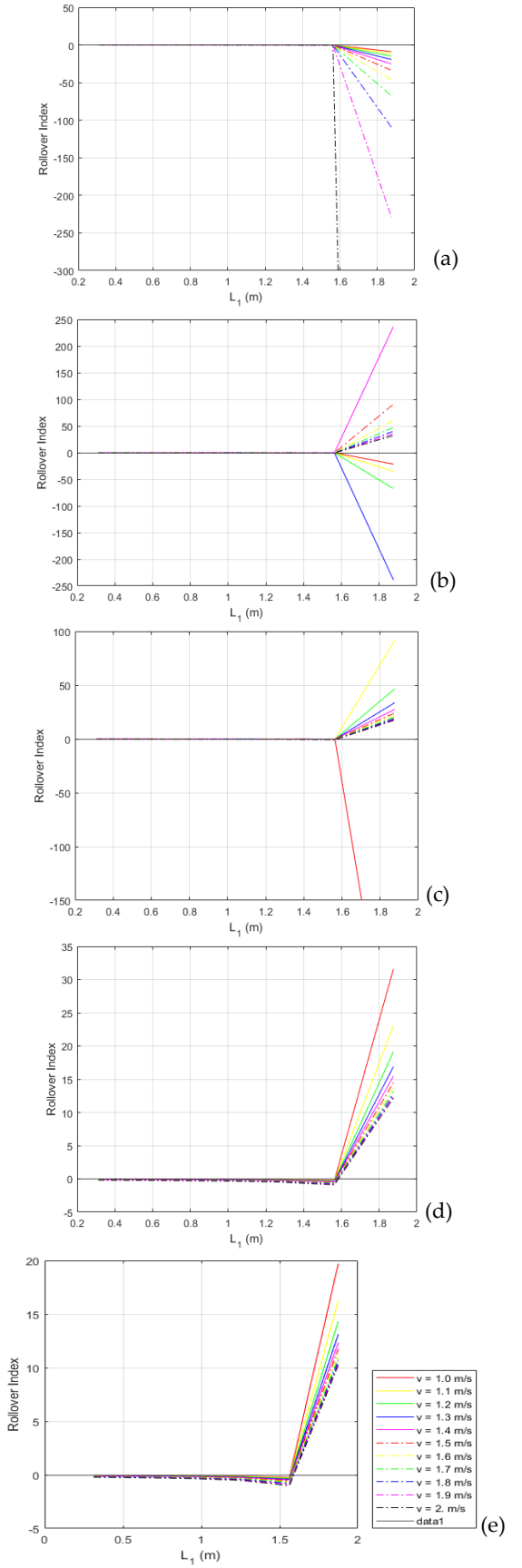

Figure 7. Rollover Index vs. L_1 for (a) $\delta = 10^{\circ}$; (b) $\delta = 15^{\circ}$; (c) $\delta = 20^{\circ}$; (d) $\delta = 25^{\circ}$; (e) $\delta = 28^{\circ}$

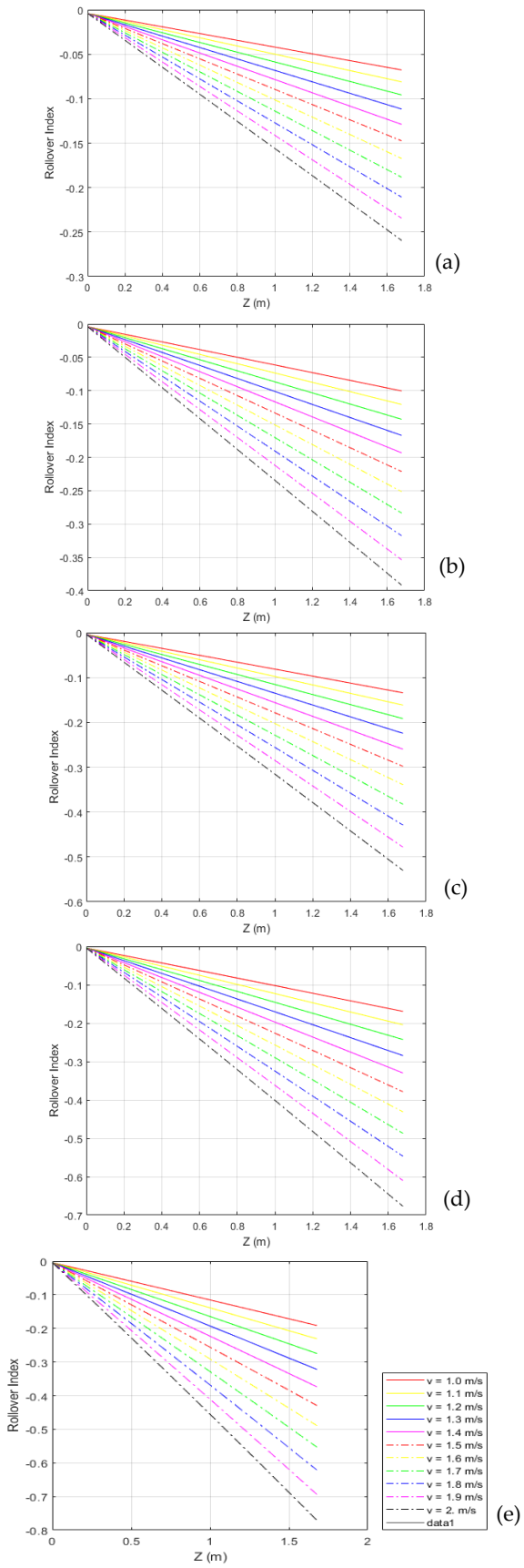

Figure 8. Rollover Index vs. Z for (a) $\delta = 10^{\circ}$; (b) $\delta = 15^{\circ}$; (c) $\delta = 20^{\circ}$; (d) $\delta = 25^{\circ}$; (e) $\delta = 28^{\circ}$

3.3. Layout Design Optimization

3.3.1. Suggested Layout Design

In this section, the layout design optimization of E-Trike is done. The optimization is used to move the center of gravity of E-Trike to the suggested location as close as possible. Since the center of gravity location correlates with the mass distribution within the E-trike, the layout design optimization is done by rearranging the powertrain components of the E-trike with respect to the layout assessment.

The first component to be relocated is the electric motor. As shown in **Figure 9**, the electric motor is initially located on the swing arm. This position allows the universal joint to operate at a similar angle all the time. However, the movement of the swing arm can cause vibration on the electric motor, and as stated in Section 2.2.3, this can cause the motor to experience premature failure. Other than that, the heavy electric motor increases the rear unsprung mass of E-Trike which would affect its handling. Thus, the electric motor should be placed on a structure that has minimum vibration. The proposed arrangement is to put it on a fix surface, i.e., on the chassis below the driver's seat. Since both shafts of the rotor and the differential are fixed, the single universal joint is no longer suitable for this arrangement. Therefore, for this arrangement, a double universal joint is used. Double universal joint allows the electric motor to transmit the torque into the differential even though they have parallel misalignment. **Figure 10** shows the mechanism of double universal joint that can compensate the parallel misalignment.

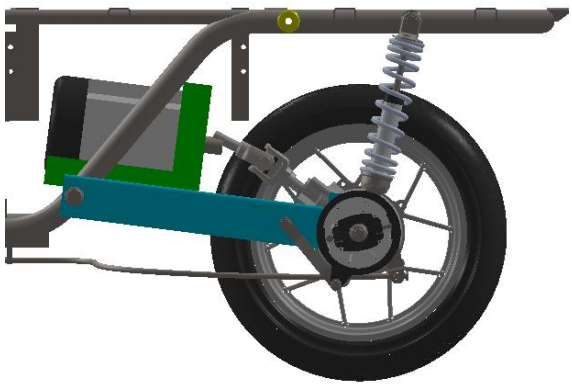

Figure 9. Initial location of the electric motor

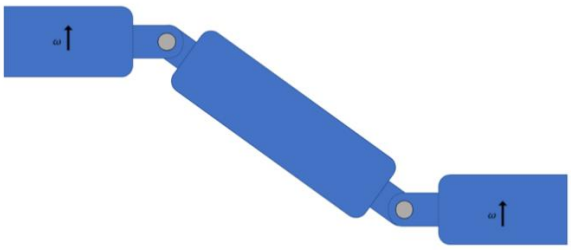

Figure 10. Double universal joint compensates the parallel misalignment.

For BMS and inverter, they need a good air circulation to optimize their work. Thus, it is good to keep them hanging on the chassis. Since they have different mass, considering the targeted center of gravity, they are hanged at the center of the chassis. **Figure 11** shows the placement of BMS and inverter before and after rearrangement.

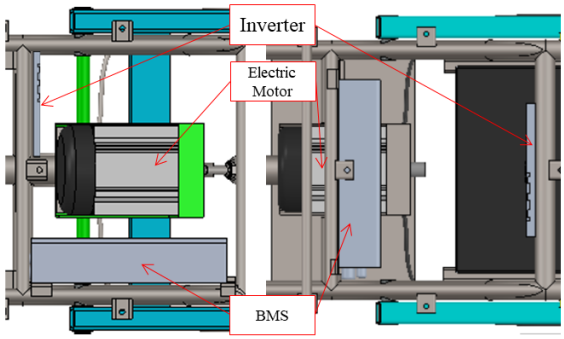

Figure 11. Initial (left) and new (right) placement for BMS, inverter, and electric motor.

Last but not least, the rearrangement on the battery pack is needed since it contributes to the mass distribution the most compared to other components. When the electric motor is rearranged, it is moved forward so that it can be placed on a fix surface, that is on the chassis below the driver's seat. However, this location is used to place the battery on the original arrangement. Thus, the battery must be moved to a new location (**Figure 12**). The only possible location for the battery is at the rear part of the E-Trike. This position has two advantages: (i) it helps to move the center of gravity of E-Trike to the rear (minimizing L_1) and (ii) the rear part of E-Trike has better air circulation, so it minimizes the possibility of thermal runaway of the battery. To compensate the vibration that the battery might experience at the rear part, additional structure must be designed on the chassis to support the battery pack. This will be done in our future study.

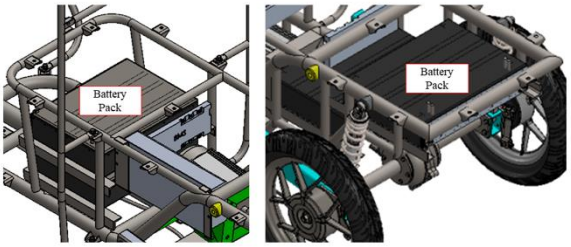

Figure 12. Battery pack location before (left) and after (right) the rearrangement.

3.3.2. *Advantages of the Proposed Layout*

Figure 13 shows the full image of the E-trike layout before and after the rearrangement.

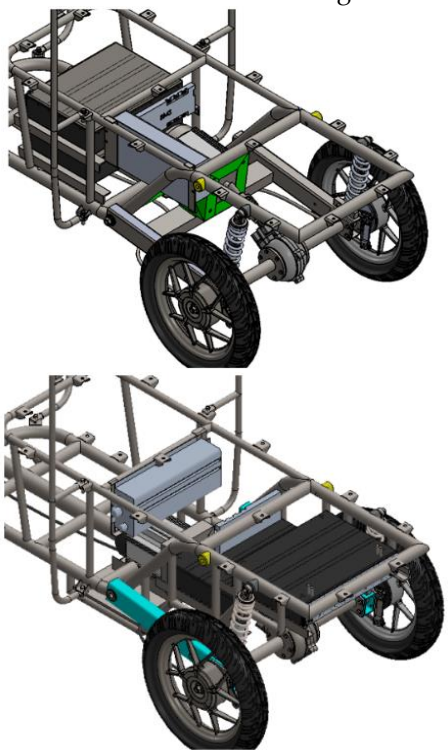

Figure 13. The E-trike's layout before (top) and after (bottom) rearrangement.

Based on **Figure 13**, a new center of gravity for the delta E-trike is obtained. The comparison between the initial and new center of gravity location is tabulated in **Table 3**. Then, a comparative analysis is done on both layout, which is shown in **Figure 14**. **Table 4** shows the effect on the new center of gravity on the turning velocity of the E-trike.

Table 3. Comparison between initial and new layout's center of gravity.

Layout	Center of Gravity Location		
	T_1 (m)	L_1 (m)	Z (m)
Initial	0.3912356	0.822893	0.6353266
New	0.4	0.7126521	0.5981451

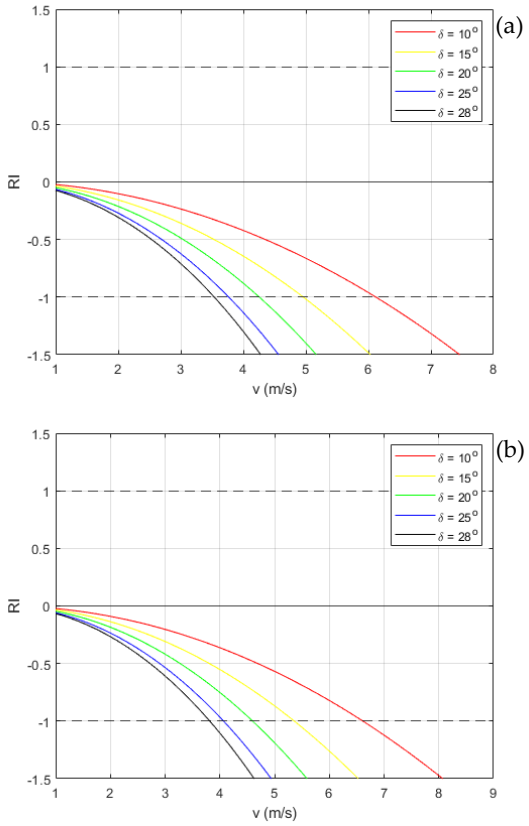

Figure 14. (a) Rollover index vs. turning velocity using initial center of gravity; (b) Rollover index vs. turning velocity using new center of gravity

Table 4. Comparison and increment percentage of the E-trike's velocities during a turn.

δ (deg.)	v_{in} (m/s)	v_{new} (m/s)	Increment (%)
10	6.05	6.6	9.090909
15	4.94	5.35	8.299595
20	4.25	4.6	8.235294
25	3.76	4.05	7.712766
28	3.52	3.82	7.954545

Table 4 shows that the new layout increases the turning velocity of the E-trike by 7.95% to 9.09%. Even though the changes are considered small, having the new layout employed on the E-trike would be worth it because of its advantageous in the consideration of component placement. In addition to increasing the turning velocity, the new layout has the following advantages:

1. It prevents the electric motor from premature failure due to vibration at the swing arm.
2. It provides better air circulation for the BMS, inverter, and battery pack, which can prevent them from overheating that can cause performance degradation or even thermal runaway.

The analysis above is performed using the curb mass of the E-trike. When the mass of the driver (70 kg) and the goods (230 kg) are included, assuming that both are at the center of the E-trike in the lateral direction, the center of gravity goes further to the front and gets higher due to the mass distribution (L_1 and Z are larger). Thus, according to **Figure 7** and **Figure 8**, the allowable turning velocity of the E-trike with the original layout lies between 2.74 m/s to 4.72 m/s. Using the new layout, the allowable turning velocity of the E-trike lies between 3.3 m/s to 5.7 m/s. The new layout increases the turning velocity by 20% for all turning angles.

The turning velocity of the E-trike has a crucial connection to the centrifugal force. The small allowable turning velocity indicates that a small centrifugal force can tip the E-trike over. It shows how prone the E-trike is to rollover. This result is also supported by the result from Austin et al. They stated that the stability of a delta tricycle is affected by the amount of the side load, which depends on the turning velocity value.

4. Conclussion

In this study, a new approach on rollover stability analysis is proposed by considering the real configuration of centrifugal force for rollover index derivation. Then, an analysis on the effect of center of gravity location or T_1, L_1, and V value on rollover index is done. In line with this analysis, a new center of gravity location is proposed. With respect to the proposed center of gravity location and layout design consideration, a rearrangement within the powertrain components is done. A comparative study between the initial and new arrangement shows that the new one can increase the turning velocity that the E-trike can have by 7.95—9.09%. It also provides a better environment for the powertrain components inside the E-trike. The effect of the suspension is not considered in our analysis. This will be an interesting future work from our study.

Acknowledgement

This research is funded by the Indonesia Endowment Fund for Education (LPDP) under Research and Innovation Program (RISPRO) for electric vehicle development with contract no. PRJ-85/LPDP/2020 and Center of Research and Community Service (CRCS) of Sampoerna University.

Author's Declaration

Authors' contributions and responsibilities

Conceived and designed the numerical experiments (F.E., D.W.D.); Performed the numerical experiments (F.E.); Analyzed and interpreted the data (D.W.D., F.E.); Wrote the original paper (F.E.); Wrote the revised manuscript (D.W.D., F.E.); Read and approved the final manuscript (D.W.D., F.T., B.A.B.).

Funding

This research is funded by the Indonesia Endowment Fund for Education (LPDP) under Research and Innovation Program (RISPRO) for electric vehicle development with contract no. PRJ-85/LPDP/2020 and Center of Research and Community Service (CRCS) of Sampoerna University.

Availability of data and materials

All data are available from the authors.

Competing interests

The authors declare no competing interest.

Additional information

No additional information from the authors.

References

[1] H. Shaftel, "Overview: Weather, global warming and climate change," *NASA*, 2021. https://climate.nasa.gov/resources/global-warming-vs-climate-change/.

[2] United Nations, "Paris Agreement," 2018. [Online]. Available: https://www.un.org/en/climatechange/paris-agreement.

[3] EPA, "Global Greenhouse Gas Emissions Data," 2017. [Online]. Available: https://www.epa.gov/ghgemissions/global-greenhouse-gas-emissions-data.

[4] H. Ritchie, "Cars, planes, trains: where do CO2 emissions from transport come from?," 2020. [Online]. Available: https://ourworldindata.org/co2-emissions-from-transport.

[5] "Car Emissions and Global Warming," *Union of Concerned Scientists*, 2014. https://www.ucsusa.org/resources/car-emissions-global-warming#:~:text=Car Emissions and Global Warming&text=Our personal vehicles are a,for every gallon of gas.

[6] "Presidential Regulation 55:2019 on Electric Vehicles," 2019. [Online]. Available:

https://policy.asiapacificenergy.org/node/3977.

[7] "Bright Future for Electric Vehicle Industry in Indonesia," *Karawang New Industry City (KNIC)*, 2021. https://www.knic.co.id/bright-future-for-electric-vehicle-industry-in-indonesia.

[8] "Indonesia Battery Corporation - Official Web Site." https://www.indonesiabatterycorporation.com/.

[9] A. Toanchina, "A View of urban vehicle," *J. Ind. Des. Eng. Graph.*, vol. 14, no. 2, 2019.

[10] M. Ataei, A. Khajepour, and S. Jeon, "Reconfigurable Integrated Stability Control for Four- and Three-wheeled Urban Vehicles With Flexible Combinations of Actuation Systems," *IEEE/ASME Trans. Mechatronics*, vol. 23, no. 5, pp. 2031–41, 2018.

[11] Kinetics, "Tadpole or delta trike?," *Kinetics*, 2016. https://www.kinetics-online.co.uk/technical-info/tadpole-or-delta-trike/.

[12] N. Rice, "6 Factors Involved in Rollover Accidents," *LLP*, 2019. https://nagelrice.com/motor-vehicle-accidents/6-factors-involved-rollover-accidents/.

[13] E. Austin, A. S. Christopher, O. Peter, E. W. Saturday, and D. D. E, "Determination of Center of Gravity and Dynamic Stability Evaluation of a Cargo-type Tricycle," *Am. J. Mech. Eng.*, vol. 3, no. 1, pp. 26–31, 2015.

[14] Z. Jin, J. Li, Y. Huang, and A. Khajepour, "Study on Rollover Index and Stability for a Triaxle Bus," *Chinese J. Mech. Eng.*, vol. 32, no. 64, 2019, doi: https://doi.org/10.1186/s10033-019-0376-0.

[15] C. Iclodean, B. Varga, N. Burnete, D. Cimerdean, and B. Jurchiș, "Comparison of Different Battery Types for Electric Vehicles," 2017, doi: https://doi.org/10.1088/1757-899x/252/1/012058.

[16] S. Cummings, "Energy storage: Preventing thermal runaway before it begins," *Power Engineering*, 2020. https://www.power-eng.com/energy-storage/energy-storage-preventing-thermal-runaway-before-it-begins/#gref.

[17] ACORN, "5 Causes of Motor Failure and How to Prevent Them," *ACORN*, 2018. https://www.acorn-ind.co.uk/insight/five-causes-of-motor-failure/.

[18] VARTA Battery World, "Battery replacement," 2018. https://batteryworld.varta-automotive.com/en-be/car-battery-replacement.

[19] "Changing the Battery Position in Electric Vehicles Could Help Boost Vehicle Range, Here's How," *News18*, Jun. 10, 2021.

[20] Gaadiwaadi, "Ground clearance of cars in india - complete list," *Gaadiwaadi.com*, 2017. https://gaadiwaadi.com/ground-clearance-of-cars-in-india-complete-list/.